Materials Letters 141 (2015) 248–251

Contents lists available at ScienceDirect

Materials Letters

journal homepage: www.elsevier.com/locate/matlet

Synthesis of pure-phase Sr_2MgMoO_6 nanostructured powder by the combustion method

Paola K. Dager [a], Corina M. Chanquía [a,b], Liliana Mogni [a,b], Alberto Caneiro [a,b,*]

[a] Centro Atómico Bariloche (CAB), Comisión Nacional de Energía Atómica (CNEA), Av. Bustillo 9500, S.C. de Bariloche CP 8400, Argentina
[b] Consejo Nacional de Investigaciones Científicas y Técnicas (CONICET), Av. Rivadavia 1917, C1033AAJ Buenos Aires, Argentina

ARTICLE INFO

Article history:
Received 2 September 2014
Accepted 11 November 2014
Available online 24 November 2014

Keywords:
Sr_2MgMoO_6
Nanostructured powder
Combustion synthesis

ABSTRACTS

Pure-phase Sr_2MgMoO_6 (SMMO) nanopowder was obtained by combustion synthesis (CS) from an aqueous solution of metal nitrates, glycine and ammonium nitrate and subsequent treatment in air at 900 °C. The morphological and structural characterization was performed by X-Ray diffraction (XRD), N_2 physisorption and scanning electron microscopy (SEM).

This nanostructured powder presents average crystallite size of ~150 nm and a sponge-like morphology composed of highly interconnected crystallites and an effective specific area of 5.6 m^2/g.

EIS measurements indicate ASR values as low as 0.07 Ω cm^2 at 800 °C.

1. Introduction

Solid Oxide Fuel Cells (SOFCs) are electrochemical devices that directly convert chemical into electrical energy with high efficiency [1,2]. Particularly, the search of new anode materials for SOFC is focussed on mixed conductors which must be compatible thermally and chemically with the other components of the cell, stable under reducing atmospheres and, able to fully oxidize different hydrocarbons. One of the promising materials as anode of SOFC is Sr_2MgMoO_6 double perovskite [2], which has been synthesized by solid state reaction, sol–gel route and freeze-drying precursors [3–9]. These process generally require temperatures higher than 1200 °C during prolonged times ($t > 20$ h) and in some cases subsequent heat treatments under diluted H_2 atmospheres [3,6,10].

An alternative to these methods is the CS [11–13] which involves the exothermic decomposition of a fuel and oxidizers generating highly reactive nano-oxides. In the present study, we report the synthesis and characterization of nanostructured Sr_2MgMoO_6 powder obtained by CS at temperature as low as 900 °C in air. To the best of our knowledge, this method has been used to obtain different types of anodes [14,15] but it has not been reported for the synthesis of Sr_2MgMoO_6 so far.

2. Experimental

Synthesis: Sr_2MgMoO_6 was synthesized by CS by employing glycine ($C_2H_5NO_2$) as fuel and complexing agent, and ammonium nitrate (NH_4NO_3, named AN) as trigger to promote the combustion process [14]. In a typical procedure to obtain 1 g of SMMO, stoichiometric amounts of $SrCO_3$ and metallic Mg (Alfa Aesar, >99%) were dissolved in a diluted HNO_3 solution, whereas MoO_3 (Mallinckrodt, 99.5%) was dissolved in NH_4OH solution. The solution was heated at $T \sim 75$ °C during 24 h. Then, distilled water (~100 mL), and different glycine and AN contents were added to a starting batch. These transparent nitrate solutions were placed in an "electric heating mantle" and kept at 150 °C for 4 h, then later the temperature increased to 180 °C. During the final stage of the evaporation, the solution began to swell forming viscous foam, and subsequently followed by the autoignition.

The ratio between the total valences of the fuel ($C_2H_5NO_2$) and the total valences of the oxidizers (nitrates) is named stoichiometric coefficient, φ [11–14], whereas R is the mass ratio between AN and glycine. These two parameters can be adjusted in order to obtain single phase materials at low synthesis temperatures. φ and R parameters were varied between 1.4–5.6 and 0.25–1.00, respectively and thermal treatments (TT) in air were performed between 700 and 1000 °C during periods of 6 and 12 h.

Characterization: XRD data were collected by using a Panalytical Empyrean equipment with Cu Kα radiation ($\lambda = 0.1542$ nm), range between $10° \leq 2\theta \leq 115°$, and scanning step of 0.026°. Specific surface area and pore size distribution were measured from N_2 physisorption isotherms obtained at 77 K in a Micromeritics ASAP 2020 instrument. The morphology of the samples was observed by

* Corresponding author at: Centro Atómico Bariloche (CAB), Comisión Nacional de Energía Atómica (CNEA), Av. E. Bustillo 9500, 8400 San Carlos de Bariloche, Argentina. Tel./fax: +54 29 4444 5274.
E-mail address: caneiro@cab.cnea.gov.ar (A. Caneiro).

http://dx.doi.org/10.1016/j.matlet.2014.11.037
0167-577X/

means of a SEM-FEG FEI NovaNano SEM 230. Electrochemical impedance spectroscopy (EIS) measurements were performed by using a symmetrical cell built with a dense $Ce_{0.95}Gd_{0.10}O_{1.95}$(CGO) electrolyte and porous SMMO electrodes deposited by spin coating [14].

3. Results and discussion

Firstly, SMMO samples were synthesized varying φ within the range $1.4 \leq \varphi \leq 5.6$. The so-obtained powders were calcined at 1000 °C for 6 h. The XRD patterns (not shown here) mainly indicated the Sr_2MgMoO_6 phase in all the samples, but with the presence of secondary phases, such as, $SrMoO_4$, SrO, MgO, $MgCO_3$and a non-identified compound at $\theta = 30.6°$. The minimum amount of these secondary phases were obtained for $\varphi = 2.8$. In view of these results, we evaluated the addition of AN to the solution containing the nitrates and glycine, fixing φ at 2.8 and varying R between 0.25 and 1.00.

In Fig. 1(a) are shown the XRD patterns of SMMO powders obtained for two optimums R values and calcined at 900 and 1000 °C for 6 h. It can be observed that single phase materials can be obtained at 1000 °C for both R values. The synthesis at 900 °C shows the presence of impurities phases for both R values with a minimum amount of the non-identified phase for $R = 0.75$. In view of these results, we fixed R at 0.75 and increased the time of TT to 12 h in order to completely remove impurity phases and explore the SMMO synthesis at lower temperatures.

In Fig. 1(b) are shown the XRD patterns of SMMO samples with $\varphi = 2.8$, $R = 0.75$, calcined between 700 and 1000 °C for 12 h, as well as the combustion product. In the inset of this figure a magnification of 2θ between 25° and 35° is shown.

At 700 °C, mainly SMMO phase is present but with two impurities: $SrMoO_4$ and the non-identified compound. Increasing the TT at 800 °C, the SMMO phase crystallizes almost completely with only $SrMoO_4$ as secondary phase: the amount of $SrMoO_4$ determined by Rietveld refinement is approximately 4%. As it can be observed, just at 900 °C pure-phase SMMO is obtained. Additionally, when the TT is increased to 1000 °C, the purity of the SMMO phase is preserved, but the narrowing of the diffraction peaks indicates crystallite growth.

The crystallite size and lattice parameters of the SMMO powder calcined at 900 and 1000 °C for 12 h were determined by Rietveld refinement of the XRD data [16] with FULLPROF program [17] by using the triclinic $I\bar{1}$ space group according to the model proposed by Bernuy-Lopez et al. (ICSD Collection code no. 173121) [3]. The refinement results are summarized in Table 1.

For SMMO powder, the average crystallite sizes were 150 and 230 nm for samples treated at 900 and 1000 °C during 12 h, respectively.

Table 1
Structural and morphological parameters of SMMO samples synthesized with $\varphi = 0.28$, $R = 0.75$ and calcined at 900 and 1000 °C during 12 h.

Parameter	Calcined temperature	
	900 °C	1000 °C
a (Å)	5.5879(7)	5.5762(4)
b (Å)	5.5881(7)	5.5753(4)
c (Å)	7.9277(1)	7.9258(1)
α	89.991(9)	89.995(7)
β	90.00(1)	89.984(5)
γ	89.981(6)	89.997(5)
V (Å3)	247.55(4)	246.40(2)
R_{wp}(%)	8.79	9.64
R_{Bragg}(%)	2.50	2.85
χ^2	2.924	3.307
Crystallite size (nm)	150	230
S_{BET} (m^2/g)	5.6	4.6

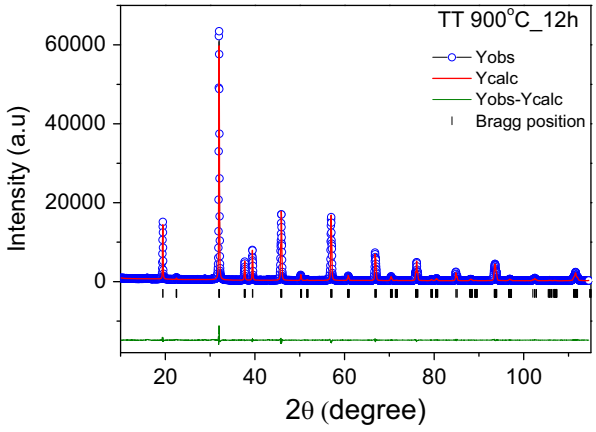

Fig. 2. Rietveld refinement profiles of SMMO calcined for 12 h at 900 °C.

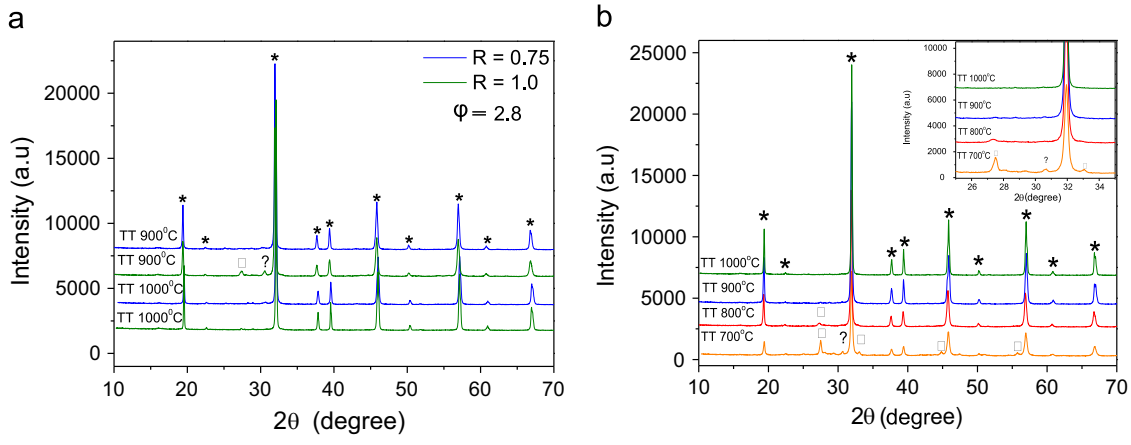

Fig. 1. XRD patterns of SMMO synthesized with $\varphi = 2.8$ varying R and TT in air. (a) $R = 0.75$ and 1.0, TT = 900 °C and 1000 °C for 6 h; (b) $R = 0.75$, 700 °C ≤ TT ≤ 1000 °C for 12 h. Present phases: *SMMO, □$SrMoO_4$,? Non-identified compound.

The obtained R_{Bragg}, R_{wp} and χ^2 values for these parameters indicated that the refinement results are acceptable.

Fig. 2 shows the refinement of the XRD data for the Sr_2MgMoO_6 nanopowder prepared with $\varphi=2.8$, $R=0.75$ and calcined at 900 °C during 12 h.

Fig. 3 displays preliminary EIS measurements performed on SMMO/CGO/SMMO cell at 500, 600, 700 and 800 °C under wet Ar-20%H_2. In the inset is shown a plot of Log(ASR) vs. 1000/T. The ASR (Area Specific Resistance) at 800 °C indicates a value of 0.07 Ω cm^2 which is 5 times lower than that of Ref. [18].

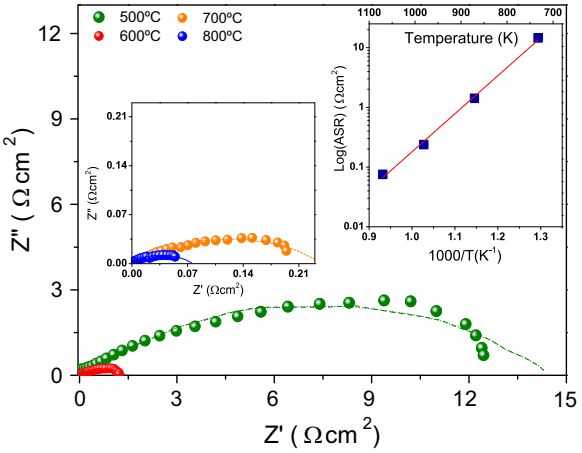

Fig. 3. EIS data of SMMO/CGO/SMMO cell at 500, 600, 700 and 800 °C. Inset: plot of Log(ASR) vs. 1000/T.

N_2 physisorption isotherms of SMMO samples synthesized with $\varphi=0.28$ and $R=0.75$ and calcined at 900 and 1000 °C for 12 h showed a specific surface area of 5.6 and 4.6 m^2/g, respectively (see Table 1). This behavior is related to the densification of the sample and a crystallite growth, as observed by XRD.

Fig. 4 shows SEM micrographs of the SMMO samples synthesized with $\varphi=0.28$ and $R=0.75$ calcined at 900 °C (a, b) and 1000 °C (c, d) during 12 h. Both samples present *highly interconnected crystallites* (particle) with a porous morphology, which is attributed to the release of large amount of gases during the combustion process. Although, the SMMO powder calcined at 1000 °C displays larger particles than those calcined at 900 °C, the crystallite sizes show a moderate variation from 150 nm (900 °C) to 230 nm (1000 °C).

4. Conclusion

Pure phase Sr_2MgMoO_6 nanopowder was synthesized by the CS after an accurate control of the synthesis parameters and thermal treatments. The optimal φ, R and the TT were 2.8, 0.75 and 900 °C for 12 h, respectively. SEM images, XRD and N_2 physisorption indicate the presence of *highly interconnected crystallites* with mainly macroporous morphology characterized by an average crystallite size around 150 nm and a specific surface area of 5.6 m^2/g. EIS measurements indicate ASR values as low as 0.07 Ω cm^2 at 800 °C. These features suggest that the SMMO materials obtained by the CS could be an efficient anode for IT-SOFC, since microstructure is essential to increase the electrode catalytic activity for the oxidation of different types of fuels.

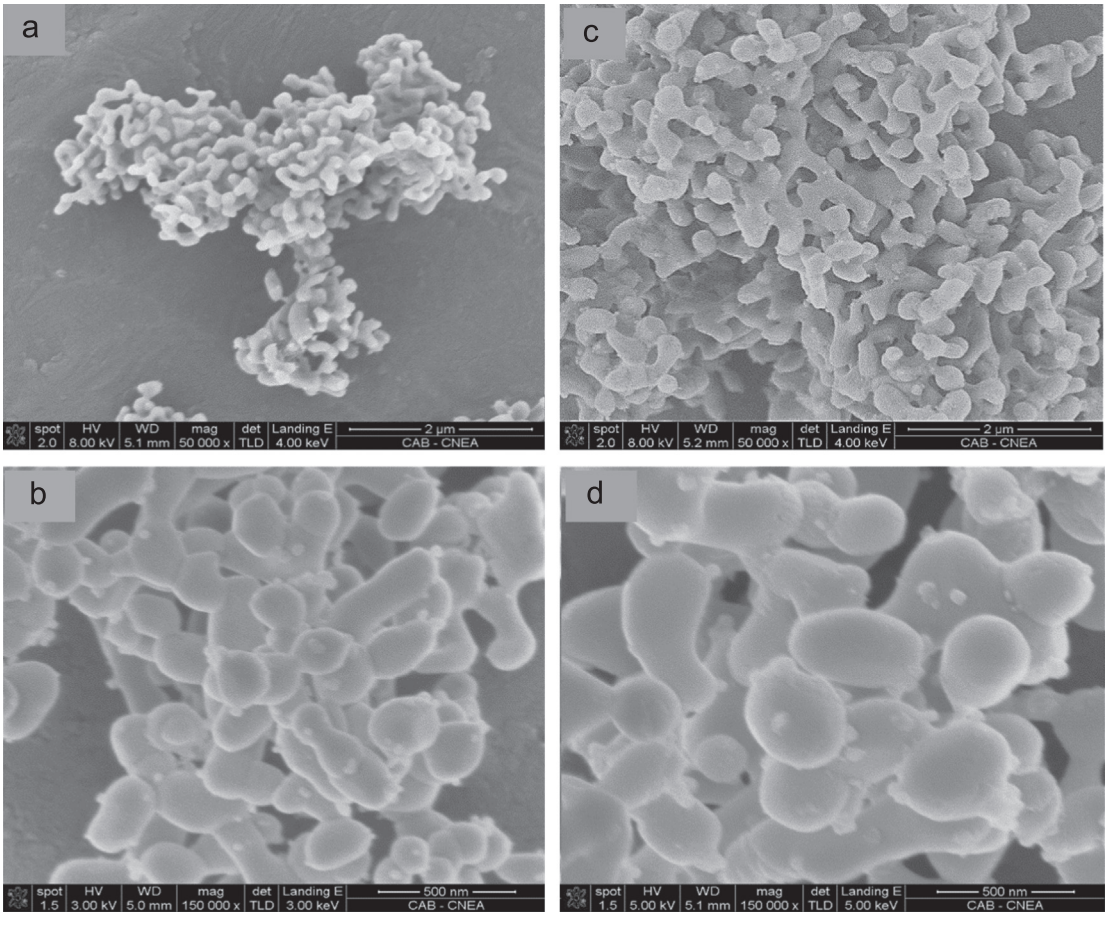

Fig. 4. SEM micrographs of SMMO samples synthesized with $\varphi=0.28$ and $R=0.75$ and calcined during 12 h at 900 °C (a, b) and 1000 °C (c, d) both with magnifications of 50k× and 150k×.

Acknowledgments

The authors kindly acknowledge the support of CNEA, CONICET and Agencia Nacional de Promoción Científica y Tecnológica (ANPCyT) to PICT 2010-0322. Special thanks to Mr. Daniel Wilberger for his valuable collaboration.

References

[1] Yokokawa H, Tu H, Iwanschitz B, Mai. A. J Power Sources 2008;182(2):400–12.
[2] Goodenough JB, Huang YH. J Power Sources 2007;173(1):1–10.
[3] Bernuy-Lopez C, Allix M, Bridges Ca, Claridge JB, Rosseinsky MJ. Chem Mater 2007;19(5):1035–43.
[4] Vasala S, Lehtimäki M, Haw SC, Chen JM, Liu RS, Yamauchi H, et al. Solid State Ionics 2010;181(15–16):754–9.
[5] Xie Z, Zhao H, Chen T, Zhou X, Du Z. Int J Hydrog Energy 2011;36(12):7257–64.
[6] Marrero-López D, Peña-Martínez J, Ruiz-Morales JC, Pérez-Coll D, Aranda MaG, Núñez P. Mater Res Bull 2008;43(8–9):2441–50.
[7] Jiang L, Liang G, Han J, Huang Y. J Power Source 2014;270:441–8.
[8] Howell TG, Kuhnell CP, Reitz TL, Sukeshini AM, Singh RN. J Power Source 2013;231:279–81.
[9] Gansor P, Xu C, Sabolsky K, Zondlo J, Sabolsky EM. J Power Source 2012;198:7–13.
[10] Vasala S, Lehtimäki M, Huang YH, Yamauchi H, Goodenough JB, Karppinen M. J Solid State Chem 2010;183(5):1007–12.
[11] Ringuede A, Labrincha JA, Frade. JR. Solid State Ionics 2001;141–142:549–57.
[12] Patil KC, Aruna T, Ekambaram. S. Curr Opin Solid State Mater Sci 1997;2:158–65.
[13] Civera A, Pavese M, Saracco G, Specchia V. Catal Today 2003;83(1–4):199–211.
[14] Chanquía CM, Montenegro-Hernández A, Troiani HE, Caneiro A. J Power Sources 2014;245:377–88.
[15] Marrero-Jerez J, Chinarro E, Moreno B, Colomer MT, Jurado JR, Núñez P. Ceram Int 2014;40:3469–75.
[16] Rietveld HM. J Appl Crystallogr 1969;2(2):65–71.
[17] Rodriguez Carvajal J. J Phys B 1993;192:55.
[18] Marrero-López D, Peña-Martínez J, Ruiz-Morales JC, Gabás M, Núñez P, Aranda MaG, et al. Solid State Ionics 2010;180:1672–82.